



## Numerical investigation of the performance of parabolic trough solar collector utilizing nanofluids as working fluids

<sup>1</sup>Hamzat, A.K., <sup>2\*</sup>Omisanya, M.I., <sup>3</sup>Olawale, B.M. and <sup>4\*</sup>Asafa, T.B.

<sup>1</sup>Mechanical Engineering Department, King Fahd University of Petroleum & Minerals, Dhahran 31261, Saudi Arabia.

<sup>2</sup>School of Mechanical Engineering, Power and Energy Department, Tianjin University, 300350 Tianjin, China.

<sup>3</sup>Physics Department, King Fahd University of Petroleum and Minerals, Dhahran 31261, Saudi Arabia.

<sup>4</sup>Department of Mechanical Engineering, LAUTECH, Ogbomoso, Oyo State.

### Article info

Received: April 4, 2022

Revised: May 13, 2022

Accepted: May 19, 2022

#### Keywords:

Parabolic trough solar collector (PTSC),  
Nanofluids,  
Non-uniform heat flux,  
Numerical analysis,  
CFD,  
Solar energy

### Abstract

Parabolic trough solar collectors have been utilized to harvest solar energy for heating and power generation for ages. While several attempts have been made to improve the design and performance of these collectors, little attention has been directed towards enhancing the thermal conduction efficiency of the heat collection fluids. By adding nanofluids, a mixture of nanoparticles and base fluids, the thermal conductivity of the working fluids can be improved, and invariably the performance of the collectors can be enhanced. This paper presents a Computational Fluid Dynamics (CFD) simulation of a parabolic trough solar collector in which distilled water, CuO/water, and TiO<sub>2</sub>/water nanofluids were used as working fluids. The nanofluids were set at 5 vol.% while turbulent flow condition with non-uniform heat flux was applied at the outer surface of the receiver. At varying lengths and diameters, the heat profiles of the receiver were obtained using a general-purpose ray-tracing software (SolTrace). The results indicated 14% and 3.5% increase in the collector efficiency for TiO<sub>2</sub>/water and CuO/water nanofluids, respectively. The simulation results agreed with the existing experimental data within  $\pm 5\%$  error. In addition, the performances of the solar collector for TiO<sub>2</sub>/water and CuO/water nanofluids were higher than for pure water by 112% and 98%, respectively. It is, therefore, recommended that TiO<sub>2</sub>/water nanofluids be utilized for parabolic trough solar collectors, given the high energy demand occasioned by population explosion and COVID-19 pandemics.

## 1. Introduction

Renewable energy, such as solar power, has been extensively used as an alternative to fossil fuels to reduce over dependence on fossil fuels. Solar energy, which is free of pollution and consequently reduces greenhouse emissions and global warming, has been deployed for heating and electricity production among others [1,2]. However, solar energy has a few setbacks including unstable radiation, high capital cost, high energy storage cost, etc. Despite these, it still accounts for up to 60% of

the global's energy production, and it is expected to continue to rise in coming years [3].

Concentrating Solar-Thermal Power (CSP) technologies have expedited conversion of solar radiation, lowered initial investment costs, and enabled thermal storage capacity for power generation after sunset and during cloud cover. Among the CSP technologies, Parabolic Trough Solar Collector (PTSC) has proven to be more efficient and reliable because of its ability to absorb solar radiation and transfer it to the receiver Heat Transfer Fluid (HTF) at a

temperature up to 400°C [4,5]. A PSTC comprises an absorber tube receiver and parabolic shaped collector with axial tracking to improve efficiency. One of the significant advantages of the PSTC is the ability of its absorber tube to reduce thermal losses with HTF gaining more energy to produce electricity [6]. Studies have

lic carbides [10]. So far, both experimental and numerical studies have been conducted to study the influence of these particles on the performance of PTSC. In this regard, Jafar and Sivaraman [11] experimentally studied the impact of nanofluid and nail twisted tape on the PTSC using Al<sub>2</sub>O<sub>3</sub>/water nanofluid at 0.1 and

**Table 1: Thermo-physical properties of nanoparticles and water [25]**

Properties	Base fluid		
	(Water)	Nanoparticles (CuO)	Nanoparticles (TiO <sub>2</sub> )
$\rho(\text{kg/m}^3)$	998.2	8933	4250
$k(\text{W/m}\cdot\text{K})$	0.613	40	12
$C_p(\text{J/kg}\cdot\text{K})$	4182	385	697
$\mu(\text{N}\cdot\text{s/m}^2)$	0.001003		

focused on increasing the heat transfer coefficient of the HTF or enlarging the convective surface area of the absorber tube as a means of improving thermal performance of PTSC [7]. Most studies utilized various working fluids to modulate the performance of PTSC. Although thermal oil is largely utilized, its environmental issues and temperature limitations are major setbacks making water, nanofluids, and refrigerants suitable alternatives [8].

Recently, nanofluids-based PTSCs have attracted attention of researchers because of their rich heat-absorbing tendency and transportability [9]. Nanofluids are formed by suspending nano-sized particles into conventional fluids. For PTSC, nanoparticles are formed from metals, non-metals, ceramics, and metal-

0.3% particle volume concentrations. The results showed that both the nanofluid and the twisted tape simultaneously increased the heat transfer performance of PTSC. Vijayan and Rajasekaran [12] reported 3.9% enhanced heat transfer performance for Al<sub>2</sub>O<sub>3</sub>/water nanofluid with particle concentration of 0.5–2.5 % in the absorber of PTSC at a fixed mass flow rate and velocity. Hosseini and Dehaj [13] also observed 63.2 and 32.1% enhanced thermal efficiency when GO/water and Al<sub>2</sub>O<sub>3</sub>/water, respectively were used as nanofluids for PTSC. Subramani *et al.* [14] used TiO<sub>2</sub>/water nanofluid in PTSC at concentrations of 0.05-0.5% and different flow rates under turbulent flow regimes. The study reported enhanced heat transfer coefficient and collector efficiency of 22.76

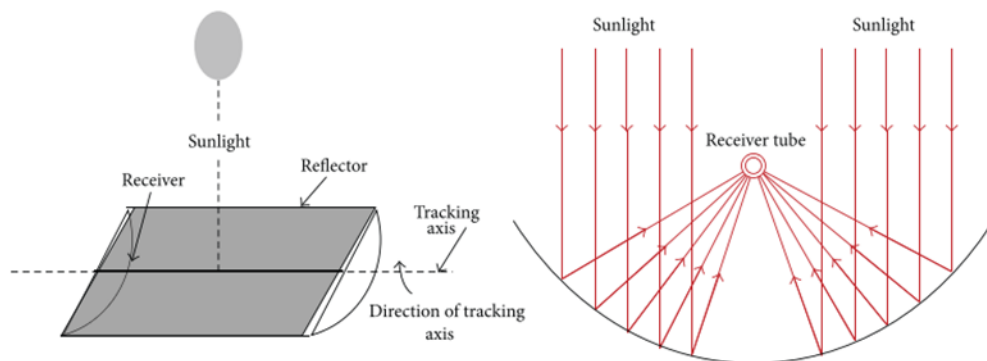


**Fig. 1: The main view and the axial diagram of the collector**

and 8.66% higher than the water-based collector. Rehan *et al.* [15] utilized both  $\text{Al}_2\text{O}_3/\text{water}$  and  $\text{Fe}_3\text{O}_4/\text{water}$  nanofluids on PTSC at three particles concentration and flow rates. The maximum efficiencies for both nanofluids were 13 and 11% at 2.0 L/min compared

proach to investigate syltherm 800/ $\text{Al}_2\text{O}_3$  nanofluid in a SEGS LS-2 module PTSC using 0-4 % volume concentration. A rise in collector efficiency of 10% was achieved at a concentration of 4%. Bellos and Tzivanidis [20] studied  $\text{CuO}/\text{syltherm 800}$  and  $\text{Al}_2\text{O}_3/\text{syltherm 800}$  nanofluids using a Eurotrough ET-150 module design PTSC with an inlet temperature of 25-325°C. Both nanofluids were compared with syltherm 800, and the results showed that  $\text{CuO}/\text{syltherm 800}$  showed the best heat transfer enhancement. Furthermore, the  $\text{CuO}$  enhanced the thermal efficiency to about 1.26%, while  $\text{Al}_2\text{O}_3$  was 1.13% when the flow rate was low, and concentration was maximum. Recently, Bellos *et al.* [21] investigated the thermal enhancement efficiency of syltherm 800/ $\text{Cu}$  nanofluid in PTSC using three collectors. The maximum enhancement was found at a low flow rate and high emissivity. An enhancement of 7.16% was achieved for a bare tube, 4.87% for a non-evacuated receiver, and 4.06% for an evacuated receiver at 25 L/min. Korres *et al.* [22] analyzed a nanofluid-based compound PTSC with Syltherm 800/ $\text{CuO}$  having a 5% nanoparticle concentration using a SolidWorks Flow Simulation Studio. Under a laminar flow regime, the examined temperature range was 25–300°C. The results showed that mean and maximum HTC was 16.16% and 17.41%, respectively while the overall enhancement efficiency was about 2.76%.

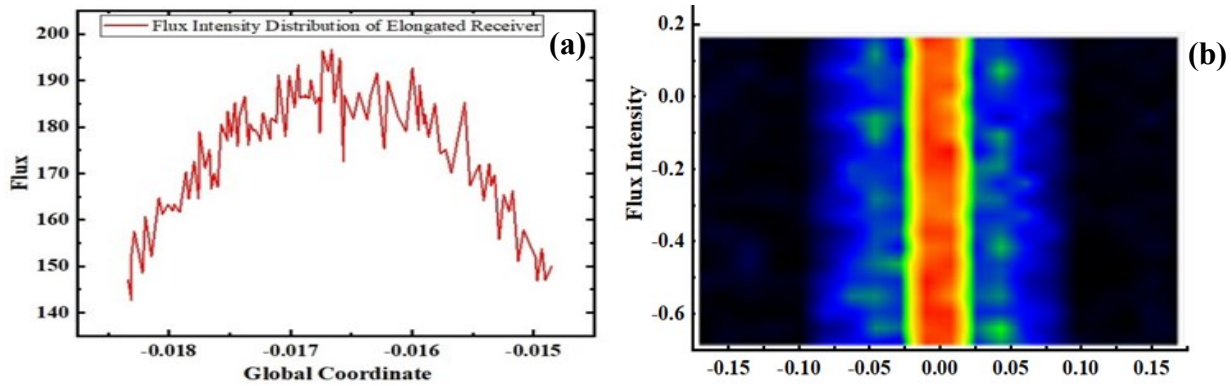


Fig. 2: Solar radiation intensity on the collector: (a) Heat distribution along the receiver (b) Contour plot for flux distribution

to water.

Many researchers have adopted numerical approaches to investigate PTSC performance instead of experimental studies to save costs and time. Mwesige *et al.* [16] used Monte Carlo ray tracing to numerically study PTSC in which single-walled carbon nanotubes were suspended in therminol VP-1. The results showed that the heat transfer performance increased by 234% while thermal efficiency rose by 4.4% at a volume concentration of 2.5%. Okonkwo *et al.* [17] investigated six different working fluids made from three nanomaterials ( $\text{CuO}$ ,  $\text{Fe}_3\text{O}_4$ , and  $\text{Al}_2\text{O}_3$ ) suspended in Therminol VP-1 using LS-2 PTSC. Of all the combinations,  $\text{Al}_2\text{O}_3/\text{Oil}$  nanofluid has the highest thermal efficiency of 0.22%. Sokhensefat *et al.* [18] numerically studied  $\text{Al}_2\text{O}_3/\text{synthetic oil}$  nanofluid in PTSC under a fully developed turbulent mixed convective heat transfer. The nanoparticle concentration, which was less than 5%, was investigated under three operating temperatures. It was found that nanoparticle concentration directly impacts the convective heat transfer coefficient of the system. Kaloudis *et al.* [19] exploited a two-phase modeling ap-

syltherm 800 nanofluids using a Eurotrough ET-150 module design PTSC with an inlet temperature of 25-325°C. Both nanofluids were compared with syltherm 800, and the results showed that  $\text{CuO}/\text{syltherm 800}$  showed the best heat transfer enhancement. Furthermore, the  $\text{CuO}$  enhanced the thermal efficiency to about 1.26%, while  $\text{Al}_2\text{O}_3$  was 1.13% when the flow rate was low, and concentration was maximum. Recently, Bellos *et al.* [21] investigated the thermal enhancement efficiency of syltherm 800/ $\text{Cu}$  nanofluid in PTSC using three collectors. The maximum enhancement was found at a low flow rate and high emissivity. An enhancement of 7.16% was achieved for a bare tube, 4.87% for a non-evacuated receiver, and 4.06% for an evacuated receiver at 25 L/min. Korres *et al.* [22] analyzed a nanofluid-based compound PTSC with Syltherm 800/ $\text{CuO}$  having a 5% nanoparticle concentration using a SolidWorks Flow Simulation Studio. Under a laminar flow regime, the examined temperature range was 25–300°C. The results showed that mean and maximum HTC was 16.16% and 17.41%, respectively while the overall enhancement efficiency was about 2.76%.

The above review indicates that harnessing solar energy via solar collectors has not been fully optimized. Therefore, more effort is still required if solar energy is to replace conventional fossil fuels in years to come. Studies have shown that the quality of heat energy produced by solar collectors depends largely on the configurations of the concentrators and receivers. As such they must be optimized for higher heat transfer. While nanofluids have been shown to enhance collector efficiency, heat transfer coefficient, and convective heat transfer in PTSC, studies have shown that most of the assumptions made are either inadequate or unrealistic. For instance, the assumption of uniform heat flux distribution is incorrect as would be demonstrated in this paper. This study reported the influence of a 5% volume concentration of CuO and TiO<sub>2</sub> nanoparticles simulated under turbulent flow conditions with non-uniform heat flux applied to the outer circumference of the absorber tube. The study also identified the best geometrical configuration for the design of the receiver tube via numerical modeling.

#### **Heat Transfer Fluid (HTF)**

Heat transfer fluid or working fluid is used to transmit energy in solar collectors. Water, a convectional base fluid, is considered the most common heat transfer fluid owing to its favorable transport properties, high heat capacity, and low cost. The thermal properties of the working fluid can be enhanced by adding nanoparticles to form nanofluids. This consequently improves the performance of solar collectors [23,24]. TiO<sub>2</sub> and CuO are used extensively in solar collectors because of their thermal and electric properties making them desirable for use as working fluids in solar collectors. For analysis, TiO<sub>2</sub> and CuO nanofluids are used as working fluid in the receiver tube of the parabolic trough solar collector, and the fluid with the best performance is identified. The volumetric concentration of the nanoparticles was set at 5% to minimize the wall temperature of

the absorber tube and also achieve a better convective heat transfer and Nusselt number. Table 1 shows the thermophysical properties of water and nanoparticles of 30 nm diameter size.

## **2.0 Description of the problem**

The schematic diagram of the parabolic trough solar collector is shown in Fig. 1. The receiver tube absorbs the solar energy and transmits it to the working fluid. To investigate the effects of the geometrical configuration of the collector receiver on solar energy harvesting, a numerical modeling approach using Computational Fluid Dynamics (CFD) analysis based on Gambit and ANSYS Fluent software is considered. The non-uniformity of the heat distribution along the receiver tube is confirmed with ray-tracing analysis carried out on the commercial software SolTrace, shown in Fig. 2. With attributes such as optical quality and graphic interfaces (Flux Map and 3D Visualization), SolTrace can be of help for simulating concentrated solar power plants (Central Receiver System, Parabolic Trough, and Dish/Stirling). The heat flux distribution data obtained from Soltrace is used as heat input in CFD analysis at a different point along the wall of the receiver. Fig. 3 shows the 2D representation of the parabolic trough solar collector receiver cross-sectional and longitudinal views with non-uniform heat flux distribution along the tube. The effect of changes in receiver length and diameter at different values of Re number using nanofluids was considered.

### **2.1 Governing equations**

For the system under study, the three-dimensional turbulent flow under a steady-state condition is governed by the continuity, momentum, and energy equation in R,  $\theta$ , and Z coordinates [26]:

The continuity equation is given in Eq. (1);

$$\nabla \cdot (\rho V) = 0 \quad (1)$$

Where  $V = (V_R, V_\theta, V_Z)$

The momentum equations are given in Eq. (2-5);

$$\nabla \cdot (\rho V V_i) = \frac{-\partial p}{\partial x_i} + \nabla \cdot (\mu \nabla V_i) + S_i \quad (2)$$

Where  $X_i = R, \theta, Z$  refer to a spatial direction.

The terms (remaining viscous terms) in equation (2) are given as follows;

For  $i = 1$ , the radial direction:

$$S_1 = \rho V_\theta \frac{V_\theta}{R} - \mu \left[ \frac{V_R}{R^2} + \left( \frac{2}{R^2} \right) \frac{\partial V_\theta}{\partial \theta} \right] \quad (3)$$

For  $i = 2$ , tangential direction:

$$S_2 = \mu \left[ \left( \frac{2}{R^2} \right) \frac{\partial V_R}{\partial \theta} - \frac{V_\theta}{R} \right] - \rho V_R \frac{V_\theta}{R} \quad (4)$$

For  $i = 3$ , the axial direction:

$$S_3 = 0 \quad (5)$$

The energy equation is depicted in Eq. (6);

$$\nabla \cdot (\rho V C_p T) = \nabla \cdot (k \nabla T) \quad (6)$$

Where  $\rho$ ,  $\mu$ ,  $k$  and  $C_p$  are the fluid density, dynamic viscosity, thermal conductivity, and specific heat, respectively. The Soltrace was used to obtain the heat flux of the parabolic trough concentrator based on the following equations [27].

The effective solar Constant was calculated by using Eq. (7);

$$I_{0,eff} = I_0 \left[ 1 + 0.033 \cos \left( \frac{360}{365.25} \right) \right] \quad (7)$$

The equation for solar declination is given in Eq. (10):

$$\delta = 23.45 \sin \left[ \frac{360}{365} (284 + n) \right] \quad (8)$$

The solar zenith angle between the vertical axis of the collector and the sun's ray direction can be calculated as;

$$\theta_z = \cos^{-1} [\sin \lambda \sin \delta + \cos \lambda \cos \delta \cos \omega] \quad (9)$$

The equation of the beam radiation under clear sky conditions;

$$I_b = I_{0,eff} \left[ a_0 + a_1 \exp \left( \frac{-k}{\cos \theta_z} \right) \right] \quad (10)$$

The ratio of beam radiation is represented by;

$$R_b = \frac{\cos \theta}{\cos \theta_z} \quad (11)$$

The solar heat flux can be calculated;

$$S = I_b R_b (\tau \alpha)_b \left( \rho \gamma + \frac{D_0}{W - D_0} \right) \quad (12)$$

## 2.2 Boundary conditions

Each region of the computational domain has a specified boundary condition. The inner region of the cylinder was assigned as a fluid. The inlet velocity was applied to all inlet boundaries as expected for incompressible fluid flow while the pressure was specified as the outlet boundary condition. More details are given in Eq. (13-14).

1. Inlet boundary condition:

The fluid flow has a uniform velocity at the receiver inlet:

$$u = U_{in}, T_f = T_{in} = 320k \text{ at } L = 0 \quad (13)$$

2. Wall boundary condition:

No-slip condition is applied on all the walls, i.e. the velocity magnitude near the wall is zero:

$$u = 0 \text{ at } r = \frac{d}{2} \quad (14)$$

Non-uniform heat flux is applied at the outer surface of the receiver with 32 different walls around the receiver wall. The flux data used in the simulation were obtained from SolTrace software.

3. A zero-pressure gradient condition is employed across the outlet boundary

## 3.0 Numerical Implementations

The governing equations were solved using the Finite Volume Method (FVM). The receiver geometry was created on GAMBIT, meshed with triangular and hybrid/tetragonal for inlet/outlet faces and volume, respectively. The grid generation for the receiver tube is shown in Fig. 4. To simulate heat transfer processes and hydrodynamics in the receiver tube, the commercial software FLUENT 19.2 was employed. All numerical solutions were

performed under the double-precision solver which outperforms the single-precision solver where temperature differences are important, and high convergence with accuracy is demanded [28].

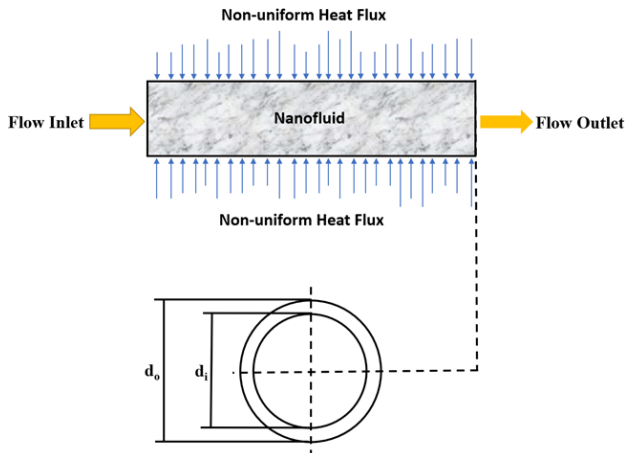


**Fig. 3:** 2D representation of parabolic trough solar collector receiver

A three-dimensional steady-state turbulence  $k-\epsilon$  RNG model with standard wall functions was used to simulate forced convection in the receiver tube. A pressure-based solver was used since the flow is incompressible. A second-order upwind was deployed to discretize the convective terms in the momentum and energy equations. However, the scheme appears to be time-consuming but yields more accurate results. The convergence criteria of  $10^{-6}$  in residuals of the continuity equation and  $10^{-9}$  in residuals of the energy equation show the solution is stable. Reynold Average Navier Stokes (RANS) equation was used to solve the momentum equation involving turbulent stresses in the chosen model. These equations are the time average equation of motion for turbulent fluid

**Table 2:** Grid independence analysis

Grid system	Grid number	Nu	%Error
Grid 1	48,000	171.57	4.10%
Grid 2	384,000	178.613	0.005%
Grid 3	3,072,000	178.622	-

flow.

### 3.1 Grid Independency

The validity and accuracy of the numerical results were carefully checked using an independent mesh analysis on the absorber

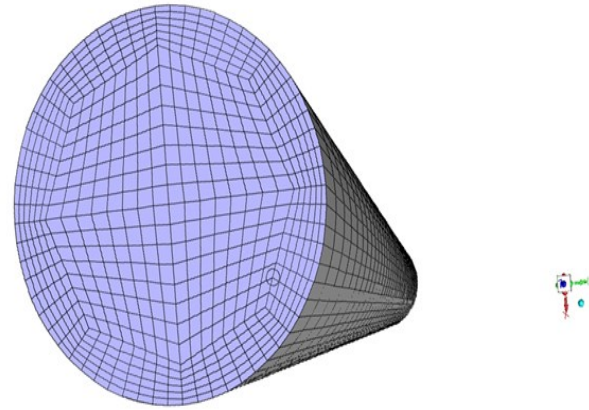


**Fig. 4:** Grid generated for parabolic trough solar collector cylindrical receiver

tube, and the Nusselt number  $Nu$  was calculated for different meshes. Three grid systems with large grid point values are considered, i.e., 48,000 cells, 384,000 cells, and 3,072,000 cells at a Reynold number  $Re$  of 30,000. The average Nusselt number on the grid systems considered is given in Table 2. It is found that the relative deviations of averaged Nusselt numbers between grid 2 and grid 3 are only 0.005%. Therefore, to reduce computational time with a high level of accuracy, the grid system of 384,000 cells was chosen. The variation of heat transfer performance represented by a Nusselt number at different Reynolds numbers is shown in Fig. 5. The Nusselt number in grid 2 and grid 3 are very close despite the difference in grid size. Therefore, grid 2 with 384,000 mesh cells saved resources and predictions accuracy for all subsequent computations.

### 3.2 Model validation

To enhance the accuracy of the model, the Nusselt number obtained from our numerical code is compared with the one estimated from the Gnielinski correlation. The Gnielinski correlation for heat transfer fluid is given by

[29]:

$$Nu = \frac{\left(\frac{f}{8}\right) (Re - 1000) Pr}{1 + 12.7 \left(\frac{f}{8}\right)^{\frac{1}{2}} (Pr^{\frac{2}{3}} - 1)} \text{ for } 3000 \leq Re \leq 5 \times 10^6 \text{ and } 0.5 \leq Pr \leq 2000$$

Where Re and Pr are Reynolds number and Prandtl number, respectively, the friction factor (f) is given as:

$$f = (0.79 \ln Re - 1.64)^{-2} \tag{16}$$

The current numerical model comparison with the Gnielinski correlation in terms of Nusselt number is shown in Fig. 6. The present model is in good agreement with the correlation for the entire range of Re numbers, and there is a maximum deviation of 4%.

In addition to the correlation agreement, further validation was conducted using CuO-

water nanofluid experimental data from Suresh et al. [30], as shown in Fig. 7. The result clearly shows an excellent agreement for the entire variation of the Re number. The validation cases concluded that k-ε RNG turbulence model and all numerical procedures used are adequate.

### 3.3 Simulation

The receiver tube of parabolic trough solar collectors was numerically simulated with variables relating to flow characteristics and thermal performance. Emphasis was placed on the heat transfer performance parameter and overall efficiency of the collector. Numerical simulation was carried out for different geometry (length and diameter) of cylindrical receivers ( $D_1 = 0.05$  m,  $D_2 = 0.07$  m,  $D_3 = 0.09$

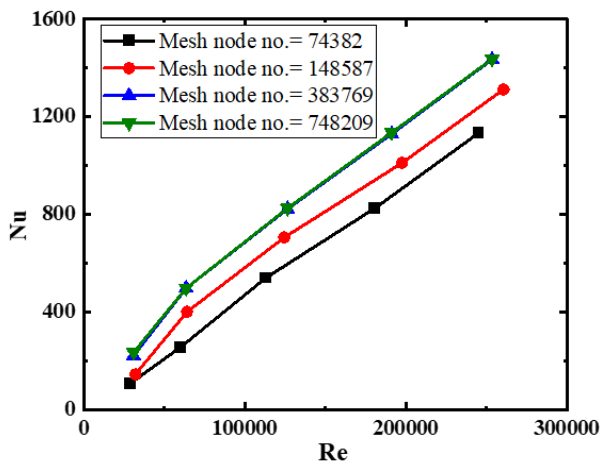


Fig. 5: Grid independence analysis for three different grids

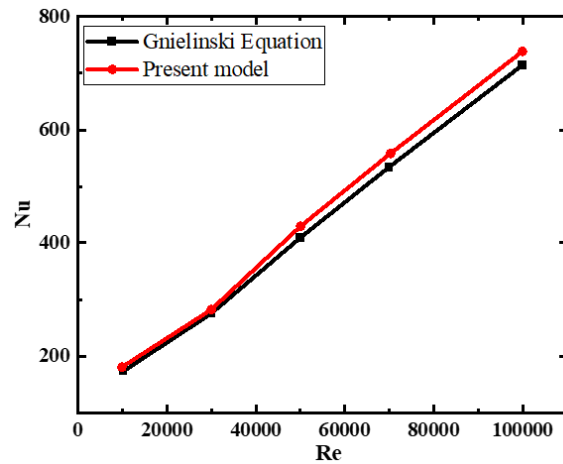


Fig. 6: Present study validation with correlations proposed by Gnielinski [29]

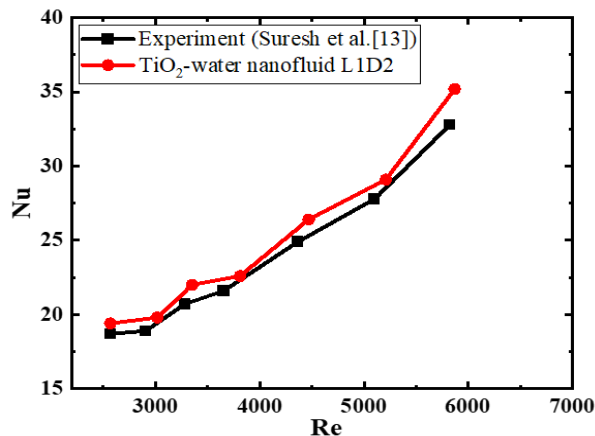


Fig. 7: Validation of present model with experimental data of CuO-nanofluid at different Reynolds number (Re)

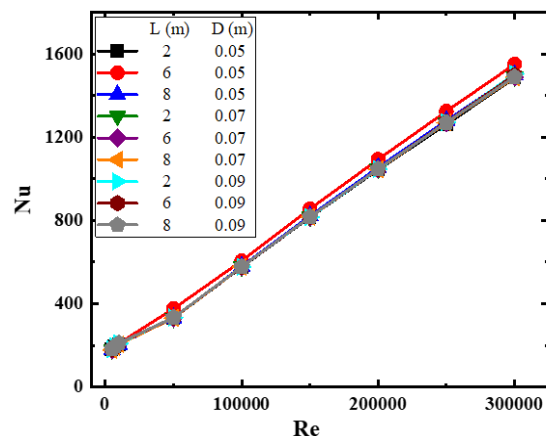


Fig. 8: Heat transfer performance at different Reynolds numbers with variation in receiver diameter

m and  $L_1 = 2$  m,  $L_2 = 6$  m,  $L_3 = 8$  m).  $TiO_2$  nanofluid was used as working fluid while heat transfer performance was studied with the variation of Nusselt number Nu number for different Reynolds numbers (5000, 7000, 10000, 50000, 100000, 150000, 200000, 250000, 300000).

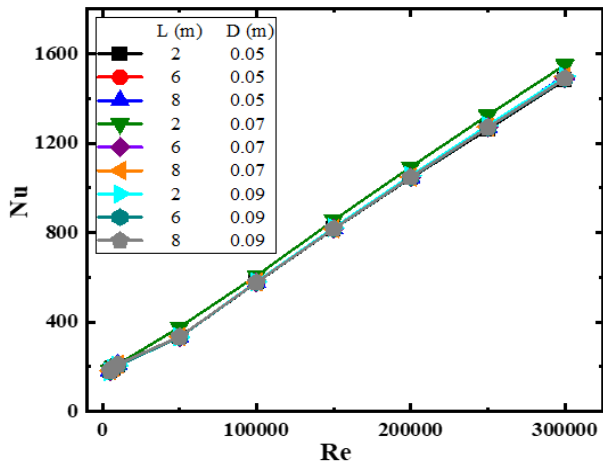


Fig. 9: Heat transfer performance at different Reynolds numbers with variation in receiver length

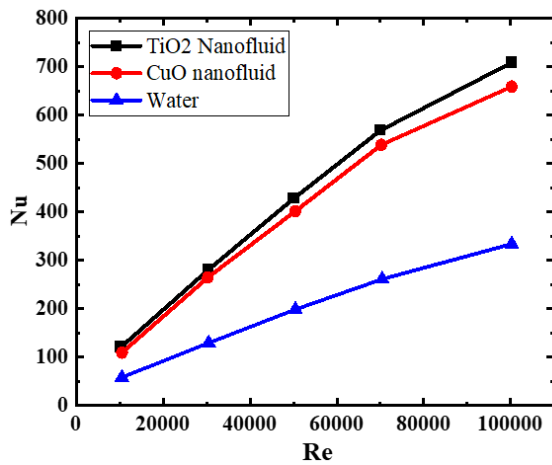


Fig. 11: Heat transfer performance for various working fluids at different Reynolds number

#### 4. Results and Discussion

The variation of the Nusselt number with Reynolds number at receiver length (2, 6, and 8 m) and diameter (0.05, 0.07, and 0.09 m) is shown in Fig. 8. It is observed that the Nusselt number increased with the Reynolds number indicating enhanced thermal performance. This is due to an increased flow velocity as the flow becomes more turbulent, favoring convective heat transfer in the collector.

Similarly, Fig. 9 shows the effect of variation of receiver length at constant diameter on the heat transfer performance of a parabolic trough solar collector. However, it appears that the two geometrical parameters do not significantly influence the heat transfer performance across various Reynolds numbers.

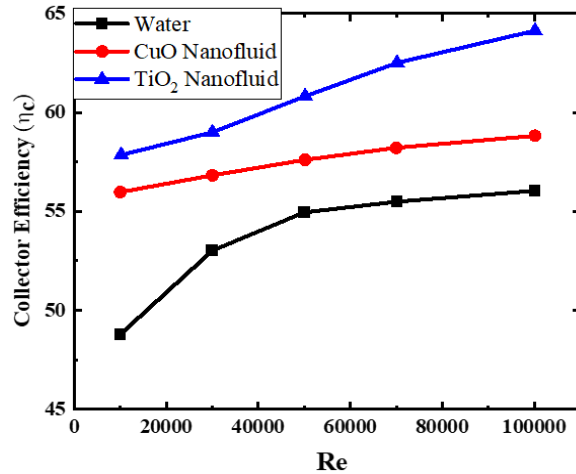


Fig. 10: Variation of collector efficiency for different working fluids with Reynolds number

These numerical simulation results save time and cost compared to the experimental setups.

Figure 10 depicts the influence of selected working fluids (Water, CuO, and  $TiO_2$  nanofluids) on the heat transfer performance of the solar collector based on the Reynolds number. From the figure, the highest Nusselt number was achieved with  $TiO_2$  nanofluid, followed by CuO nanofluid and pure water. This is largely due to the thermal conductivity of the added nanoparticles. The heat transfer performance represented by the Nusselt number increased by 112% when the heat transfer fluid was changed from pure water to  $TiO_2$  nanofluid and 98% when CuO nanofluid was deployed. The significant enhancement of collector thermal performance highlights the importance of nanofluid in solar energy harvesting. Similarly, increased mass flow rate also improved collector efficiency as displayed in Fig. 11. This indicates that a maximum collector efficiency of 14% was obtained with  $TiO_2$  nanofluid and 3.5% for CuO nanofluids compared to water. Also, higher flow rates raise Reynolds numbers leading to enhanced col-

Table 3: Comparison between existing and current studies

Authors	Method	Base fluid	Nanoparticles	Maximum Volume Concentration	Heat transfer performance (%)
Mwesigwe <i>et al.</i> [31]	CFD	Syltherm800	CuO	6 vol. %	38
Bellos <i>et al.</i> [32]	CFD	Syltherm 800	CuO	6 vol. %	130
Allouhi <i>et al.</i> [33]	Model	Therminol VP -1	TiO <sub>2</sub> , CuO, Al <sub>2</sub> O <sub>3</sub>	5 vol. %	83
Hatami <i>et al.</i> [34]	CFD	Water	Cu, Fe <sub>3</sub> O <sub>4</sub> , Al <sub>2</sub> O <sub>3</sub> , TiO <sub>2</sub>	8 vol. %	—
Current study	CFD	Water	CuO & TiO <sub>2</sub>	5 vol. %	112 & 98

lector efficiency.

Figure 12 shows the outer temperature contours at different receiver configurations across a range of Reynolds numbers. The contour is presented for TiO<sub>2</sub> nanofluid as the working fluid at a constant volume concentration of 5%. According to the nonuniform heat flux applied to the receiver tube, the highest temperature was obtained at the surface outlet

due to the solar intensity at that part of the tube. The effect of working fluid temperature on the receiver tube diminished as it moved inward. The velocity contours for various flow configuration with varying receiver geometry is shown in Fig. 13. It can be seen that the receiver tube's velocity was highest in the middle of the tube and gradually declined as it moved towards the wall, eventually falling to

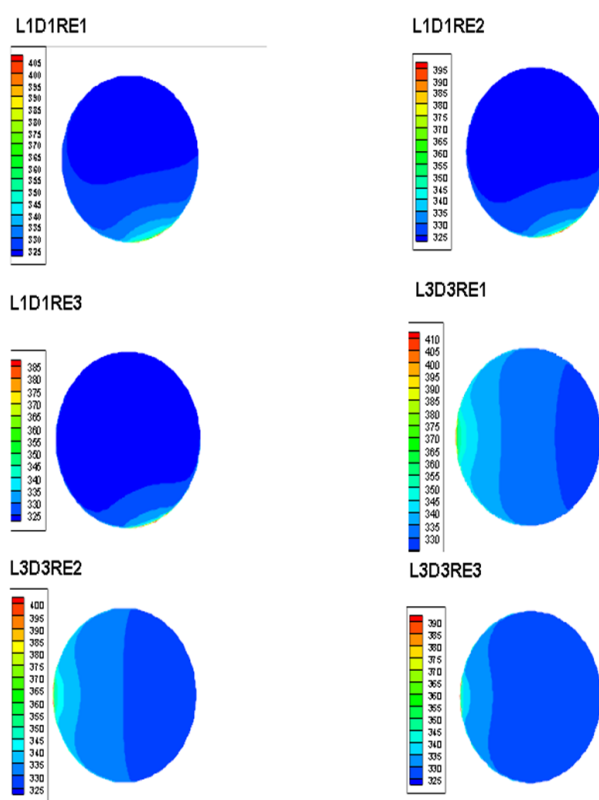


Fig. 12: Contours of Temperature for different flow configurations of the receiver geometry

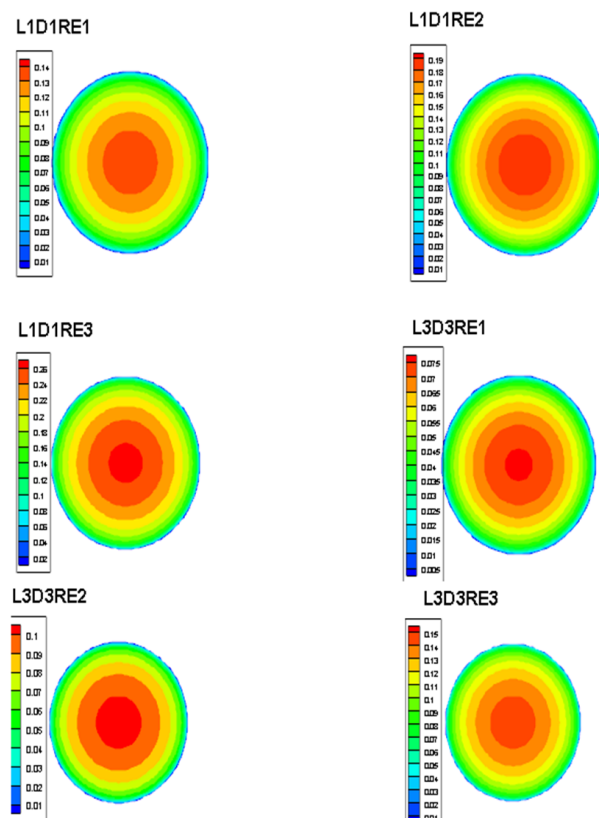


Fig. 13: Contours of velocity for different flow configurations of the receiver geometry

practically zero. The contour reflects the increase in thermal performance of the collector with an increase in flow characteristics. Also, with the utilization of nanofluid in place of pure water, the heat loss through the collector module is low. Therefore, it ensures high solar energy harvesting and is very useful to reduce greenhouse emissions. Table 3 shows the comparison between existing research and this present study. Allouhi *et al.* [33] combined TiO<sub>2</sub>, CuO, and Al<sub>2</sub>O<sub>3</sub> nanoparticles using Therminol VP-1 as base fluid at 5 vol. %. A heat transfer performance of 83% was achieved with CuO followed by TiO<sub>2</sub> and Al<sub>2</sub>O<sub>3</sub>. Using water as the base fluid in this present study, TiO<sub>2</sub> and CuO achieved heat transfer performance of 112 % and 98 %, respectively.

## 5. Conclusion

A numerical investigation was conducted to assess the performance of a parabolic trough solar collector with pure water, CuO, and TiO<sub>2</sub> nanofluids used as working fluids. A feasible non-uniform heat flux distribution along the collector receiver was applied, and the flux data was obtained from ray-tracing analysis software (SolTrace). According to the results obtained, the geometry of the receiver (length and diameter) does not significantly influence the heat transfer performance of the system. The efficiency of TiO<sub>2</sub> nanofluid is the highest, followed by CuO nanofluid and then water. Nusselt number increases with the Reynold number and maximum heat transfer is achieved under turbulent flow conditions. The highest Nu number was achieved with TiO<sub>2</sub> nanofluid, followed by CuO nanofluid and then water. The change in the Nu number was negligible at low Reynold numbers as it depicts laminar flow conditions when the convective heat transfer is low. Going forward, an economic and environmental feasibility analysis should be conducted to increase investors' confidence on the technology for commercialization. Artificial intelligence needs to be deployed in future work to normalize the variation in numerical values of

the thermophysical properties of nanofluids used during numerical analysis.

### Declaration of Competing Interest

The authors declare that they have no known competing financial interests or personal relationships that could have appeared to influence the work reported in this paper.

### Author's contributions

**HAK:** Conceptualization, Data curation, Formal analysis, Methodology, Validation, Software, Writing - original draft, Writing - review & editing.

**OMI:** Data curation, Formal analysis, Methodology, Validation, Writing - original draft, Writing - review & editing

**OBM:** Data curation, Methodology, Validation. **ATB:** Investigation, Methodology, Project administration, Supervision, Writing - original draft, Writing - review & editing.

### References

- [1] Tiwar AK, Kumar V, Said Z, Paliwal HK, 2021. A review on the application of hybrid nanofluids for parabolic trough collector: Recent progress and outlook. *J. Clean. Prod.* 292: 126031. <https://doi.org/10.1016/j.jclepro.2021.126031>.
- [2] Sandeep HM, Arunachala UC, 2017. Solar parabolic trough collectors: A review on heat transfer augmentation techniques. *Renew. Sustain. Energy Rev.* 69: 1218–1231. <https://doi.org/10.1016/J.RSER.2016.11.242>.
- [3] Olia H, Torabi M, Bahiraei M, Ahmadi MH, Goodarzi M, Safaei MR, 2019. Application of nanofluids in thermal performance enhancement of parabolic trough solar collector: State-of-the-Art. *Appl. Sci.* 9(3): 463. <https://doi.org/10.3390/app9030463>.
- [4] Mwesigye A, Meyer JP, 2017. Optimal thermal and thermodynamic performance of a solar parabolic trough receiver with different nanofluids and at different concentration ratios. *Appl. Energy.* 193: 393–413. <https://doi.org/10.1016/j.apenergy.2017.02.064>.
- [5] Amina B, Miloud A, Samir L, Abdelylah B, Solano JP, 2016. Heat transfer enhancement in a parabolic trough solar receiver using longitudinal fins and nanofluids. *J. Therm. Sci.* 25: 410–417. <https://doi.org/10.1007/S11630-016-0878-3>
- [6] [Kalogirou SA, 2004. Solar thermal collectors and applications. *Prog. Energy Combust. Sci.* 30: 231–295. <https://doi.org/10.1016/j.peccs.2004.02.001>.
- [7] Bellos E, Tzivanidis C, Antonopoulos KA, Gkinis G, 2016. Thermal enhancement of solar parabolic trough collectors by using nanofluids and converging-diverging absorber tube. *Renew. Energy.* 94: 213–222. <https://doi.org/10.1016/j.renene.2016.03.062>
- [8] Yousefi T, Veysi F, Shojaeizadeh E, Zinadini S, 2012. An experimental investigation on the effect

- of Al<sub>2</sub>O<sub>3</sub>-H<sub>2</sub>O nanofluid on the efficiency of flat-plate solar collectors. *Renew. Energy*. 39: 293–298. <https://doi.org/10.1016/j.renene.2011.08.056>.
- [9] He Q, Zeng S, Wang S, 2015. Experimental investigation on the efficiency of flat-plate solar collectors with nanofluids. *Appl. Therm. Eng.* 88: 165–171. <https://doi.org/10.1016/j.applthermaleng.2014.09.053>.
- [10] Wang Y, Xu J, Liu Q, Chen Y, Liu H, 2016. Performance analysis of a parabolic trough solar collector using Al<sub>2</sub>O<sub>3</sub>/synthetic oil nanofluid. *Appl. Therm. Eng.* 107: 469–478. <http://dx.doi.org/10.1016%2Fj.applthermaleng.2016.06.170>.
- [11] Jafar KSJ, Sivaraman B, 2015. Thermal performance of solar parabolic trough collector using nanofluids and the absorber with nail twisted tapes inserts. *Int. Energy J*, 14:189-198.
- [12] Vijayan G, Rajasekaran K, 2020 Performance evaluation of nanofluid on parabolic trough solar collector, *Therm. Sci.* 24: 853–864. <https://doi.org/10.2298/TSCI180509059G>
- [13] Hosseini SMS, Dehaj MS, 2021. An experimental study on energetic performance evaluation of a parabolic trough solar collector operating with Al<sub>2</sub>O<sub>3</sub>/water and GO/water nanofluids, *Energy*. 234: 121317. <https://doi.org/10.1016/j.energy.2021.121317>
- [14] Subramani J, Nagarajan PK, Mahian O, Sathyamurthy R, 2018. Efficiency and heat transfer improvements in a parabolic trough solar collector using TiO<sub>2</sub> nanofluids under turbulent flow regime. *Renew. Energy*. 119: 19–31. <https://doi.org/10.1016/j.renene.2017.11.079>.
- [15] Rehan MA, Ali M, Sheikh NA, Khalil MS, Chaudhary GQ, Rashid T, Shehryar M, 2018. Experimental performance analysis of low concentration ratio solar parabolic trough collectors with nanofluids in winter conditions. *Renew. Energy*. 118: 742–751. <https://doi.org/10.1016/j.renene.2017.11.062>.
- [16] Mwesigye A, Yilmaz IH, Meyer JP, 2018. Numerical analysis of the thermal and thermodynamic performance of a parabolic trough solar collector using SWCNTs-Therminol® VP-1 nanofluid. *Renew. Energy*. 119 (2018) 844–862. <https://doi.org/10.1016/j.renene.2017.10.047>
- [17] Okonkwo EC, Abid M, Ratlamwala TAH, 2018. Numerical analysis of heat transfer enhancement in a parabolic trough collector based on geometry modifications and working fluid usage, *J. Sol. Energy Eng.* 140(5): 051009. <https://doi.org/10.1115/1.4040076>
- [18] Sokhansefat T, Kasaeian AB, Kowsary F, 2014. Heat transfer enhancement in parabolic trough collector tube using Al<sub>2</sub>O<sub>3</sub>/synthetic oil nanofluid, *Renew. Sustain. Energy Rev.* 33: 636–644. <https://doi.org/10.1016/j.rser.2014.02.028>.
- [19] Kaloudis E, Papanicolaou E, Belessiotis V, 2016. Numerical simulations of a parabolic trough solar collector with nanofluid using a two-phase model, *Renew. Energy*. 97: 218–229. <https://doi.org/10.1016/j.renene.2016.05.046>.
- [20] Bellos E, Tzivanidis C, 2017. Parametric investigation of nanofluids utilization in parabolic trough collectors, *Therm. Sci. Eng. Prog.* 2: 71–79. <https://doi.org/10.1016/j.tsep.2017.05.001>.
- [21] Bellos E, Tzivanidis C, Said Z, 2020. A systematic parametric thermal analysis of nanofluid-based parabolic trough solar collectors, *Sustain. Energy Technol. Assessments*. 39: 100714.
- [22] Korres D, Bellos E, Tzivanidis C, 2019. Investigation of a nanofluid-based compound parabolic trough solar collector under laminar flow conditions, *Appl. Therm. Eng.* 149: 366–376. <https://doi.org/10.1016/j.applthermaleng.2018.12.077>.
- [23] Wadekar VV, 2017. Ionic liquids as heat transfer fluids—an assessment using industrial exchanger geometries, *Appl. Therm. Eng.* 111: 1581–1587. <https://doi.org/10.1016/j.applthermaleng.2016.04.156>
- [24] Vignarooban K, Xu X, Arvay A, Hsu K, Kannan AM, 2015. Heat transfer fluids for concentrating solar power systems—A review. *Appl. Energy*. 146: 383–396. <https://doi.org/10.1016/j.apenergy.2015.01.125>
- [25] Ögüt EB, 2009. Natural convection of water-based nanofluids in an inclined enclosure with a heat source, *Int. J. Therm. Sci.* 48 (2009) 2063–2073. <https://doi.org/10.1016/j.ijthermalsci.2009.03.014>
- [26] Yuan SW, 1967. Foundations of Fluid Mechanics, Prentice Hall, New York, USA.
- [27] Duffie JA, Beckman WA, 2006. Solar Engineering of Thermal Processes. John Wiley & Sons, Inc. <https://doi.org/10.1002/9781118671603>.
- [28] Fluent 6.3 user's guide, (2006).
- [29] Gnielinski V, 1976. New equations for heat and mass transfer in turbulent pipe and channel flow. *Int. Chem. Eng.* 16: 359–368.
- [30] Suresh S, Selvakumar P, Chandrasekar M, Raman VS, 2012. Experimental studies on heat transfer and friction factor characteristics of Al<sub>2</sub>O<sub>3</sub>/water nanofluid under turbulent flow with spiraled rod inserts. *Chem. Eng. Process.* 53: 24–30. <https://doi.org/10.1016/J.CEP.2011.12.013>.
- [31] Mwesigye A, Huan Z, Meyer JP, 2015. Thermal Performance of a Receiver Tube for a High Concentration Ratio Parabolic trough System and Potential for Improved Performance with Syltherm800-CuO Nanofluid. In Proceedings of the ASME International Mechanical Engineering Congress and Exposition, Houston, TX, USA, 13 – 19. <https://doi.org/10.1115/IMECE2015-50234>.
- [32] Bellos E, Tzivanidis C, Tsimpoukis D, 2018. Enhancing the performance of parabolic trough collectors using nanofluids and turbulators. *Renew. Sustain. Energy Rev.*, 91, 358–375. <https://doi.org/10.1016/j.rser.2018.03.091>.
- [33] Allouhi A, Amine MB, Saidur R, Kousksou T, Jamil A, 2018. Energy and exergy analyses of a parabolic trough collector operated with nanofluids for medium and high temperature applications. *Energy Convers. Manag.* 155, 201–217. <http://dx.doi.org/10.1016/j.enconman.2017.10.059>.
- [34] Hatami M, Geng J, Jing D, 2018. Enhanced Efficiency in Concentrated Parabolic Solar Collector (CPSC) with a Porous Absorber Tube Filled with Metal Nanoparticle Suspension. *Green Energy Environ.* 3, 129–137. <https://doi.org/10.1016/j.gee.2017.12.002>.